IEEE Access
Multidisciplinary ⋮ Rapid Review ⋮ Open Access Journal

Received January 27, 2020, accepted February 14, 2020, date of publication February 20, 2020, date of current version March 4, 2020.

Digital Object Identifier 10.1109/ACCESS.2020.2975316

Multi-Surrogate Collaboration Approach for Creep-Fatigue Reliability Assessment of Turbine Rotor

LU-KAI SONG AND GUANG-CHEN BAI
School of Energy and Power Engineering, Beihang University, Beijing 100191, China
Corresponding author: Lu-Kai Song (songlukai29@163.com)

This work was supported in part by the National Natural Science Foundation of China under Grant 51975028 and Grant 51575024, and in part by the Academic Excellence Foundation of BUAA for Ph.D. Students under Grant BY1604137.

ABSTRACT The creep-fatigue resistance of turbine rotor seriously affects the reliability performance and service lifetime of aircraft engine. Creep-fatigue reliability assessment is an effective measure to quantify the uncertain creep-fatigue damage and evaluate the creep-fatigue reliable life for turbine rotor. To improve the modeling accuracy and simulation efficiency of creep-fatigue reliability assessment, a multi-surrogate collaboration approach (MSCA) is proposed by absorbing the strengths of the proposed dynamic neural network surrogate (DNNS) into distributed collaborative strategy. The creep-fatigue reliability assessment of a typical turbine rotor is regarded as one case to estimate the presented MSCA with respect to the fluctuations of multi-physical variables and the variabilities of multi-model parameters. The assessment results reveal that the creep-fatigue reliable life of turbine rotor under reliability degree of 0.998 7 is 629 cycles, and the fatigue strength coefficient and holding creep time play a leading role on creep-fatigue reliable life since their effect probabilities of 27 % and 19 %, respectively. Comparison of various methods (direct Monte Carlo simulation, response surface, neural network surrogate, DNNS) shows that the presented MSCA holds high efficiency and accuracy in creep-fatigue reliability assessment of turbine rotor.

INDEX TERMS Creep-fatigue life, reliability assessment, turbine rotor, surrogate model, neural network.

I. INTRODUCTION

Modern aircraft engine tends to require high thrust-weight-ratio and superior flight safety performance [1], [2]. As a critical hot-section component of aircraft engine, the turbine rotor is often subjected to significant mechanical stresses under long-term harsh high-temperature, high-pressure and high-speed conditions [3], [4]. Consequently, the structural failure and integrity damage of turbine rotor usually pose a severe threat to reliability performance and flight security of aircraft engine [5], [6]. Creep-fatigue coupling failure is a primary failure mode, generated by the nonlinear interaction effects of low cycle fatigue damage and high-temperature creep damage, and seriously affects the reliability performance and restricts the service lifetime of turbine rotor [7], [8]. Therefore, it is crucial to effectively assess turbine rotor creep-fatigue resistance to cater for the extraordinary design requirement of aircraft engine.

The associate editor coordinating the review of this manuscript and approving it for publication was Sotirios Goudos.

Extensive efforts have been performed to predict the creep-fatigue damage and evaluate the creep-fatigue life by deterministic analyses [9]–[12], which assesses the structural integrity of turbine rotor with a reserved service lifetime. In fact, however, creep-fatigue life shows a stochastic behavior due to the following uncertain factors: material variabilities, load fluctuations, dimension variations and modeling uncertainties [13]–[15]. In this case, to quantify these multi-uncertainties and evaluate creep-fatigue reliable life, creep-fatigue reliability assessment were emerged, including strain-life fatigue modeling and simulation [16], [17], anti-fatigue reliability assessment [18], [19], creep-fatigue sensitivity analysis [20], failure-based probabilistic fatigue modeling [21], and probabilistic fatigue life estimation with DARWIN and AFGROW software [22], [23]. Among them, the dispersions or variabilities in fatigue life assessment were adequately explored, and the effectiveness of predicting fatigue reliable life were proven as well. However, it appears that these studies require thousands of nonlinear finite element (FE) calculations in evaluating the fatigue reliable life due to the application of the direct Monte Carlo simulation approach [24], [25]. For complex turbomachinery structures like turbine rotor, the direct Monte Carlo simulation approach is destinated to be unpractical owing to its huge computing amount and unacceptable computing efficiency [26]. As a result, to simplify calculation tasks and improve computing efficiency, it is urgently necessary to present a high-efficiency and high-accuracy approach for creep-fatigue reliability assessment of turbine rotor.

Under such circumstances, as valuable alternatives to direct Monte Carlo simulation, surrogate model methods were developed to lessen excess simulation tasks and widely employed into reliability assessment, sensitivity analysis and probabilistic design [27]–[30]. Typical surrogate models involve polynomial response surface [31], [32], support vector regression [33], [34], Kriging surrogate (KS) [35], [36] and neural network surrogate (NNS) [37]–[39]. By integrating flexible network topology and strong nonlinear fitting ability, NNS holds the potentials to improve the computational efficiency in performing complex reliability assessment issues. Nevertheless, for the time-varying and nonlinearity traits in the creep-fatigue reliability assessment of turbine rotor [40], [41], the usual NNS method is still insufficient to obtain satisfactory efficiency and accuracy. To the best of authors' knowledge, two key factors contribute to the defects: (1) NNS model can only approximates the performance function at a certain instant other than the whole-time domain, which consumes unaffordable computational cost in fitting each time-varying creep-fatigue responses. (2) NNS model is hard to address the complex multi-level problems (i.e., creep-fatigue reliability assessment) with high nonlinearity, which raises approximation errors and unsatisfactory accuracy.

To address the above two issues, this paper proposes a multi-surrogate collaboration approach (MSCA) to enhance efficiency and accuracy of creep-fatigue reliability assessment. In respect of the dynamic process transformation ability of time-varying traits for extremum selection mechanism [42], [43], great generalization ability of designing training cost function for Bayesian regularization (BR) theory [44], [45] and the global nonlinear convergence ability of optimal parameters for variable metric (VM) algorithm [46], [47], a dynamic NNS (DNNS) model with corresponding BR-VM error control technique is constructed. Meanwhile, the MSCA mathematical modeling and creep-fatigue reliability assessment theory are developed by employing the distributed collaborative strategy [48], [49] to further lessen nonlinearity and complexity of DNNS model. The presented MSCA is validated by the creep-fatigue life reliability assessment of a classic turbine rotor.

The paper is organized as follows: In Section 2, the authors previously present the DNNS modeling, the MSCA mathematical modeling and corresponding creep-fatigue reliability assessment theory. In Section 3, with the developed MSCA, we perform the creep-fatigue life reliability assessment of turbine rotor in respect of the multi-source uncertainties of multi-physical and multi-model parameters. Some conclusions are summarized in Section 4.

II. MULTI-SURROGATE COLLABORATION APPROACH

A. DYNAMIC NEURAL NETWORK SURROGATE

In this subsection, dynamic neural network surrogate (DNNS) model is first proposed to address the time-varying and nonlinear problems. By integrating of the feedforward neural network to build the network topology structure, extremum selection mechanism to simplify the time-varying training & testing samples, and BR-VM error control technique to train the optimal network parameters, the DNNS is mathematically modeled. Note that the DNNS model is named by its modeling traits and employment scopes.

For a reliability assessment system with the time-varying and nonlinear traits, the output responses of the assessment system are dynamic stochastic processes, which usually give rise to significant computational errors and expensive simulation cost in approximating each dynamic response.To solve the computing dilemma, a dynamic neural network surrogate (DNNS) method is proposed by transforming the multi-dimensional dynamic processes into one-dimensional maximum response with an extremum selection mechanism [42], [43] and fitting the black-box nonlinear relationships between input variables and maximum response with a neural network surrogate (NNS) model. Owing to the extremum selection mechanism only considers a maximum value rather than all of dynamic responses, the computational complexity of DNNS method can be effectively reduced. Moreover, due to the strong nonlinear fitting ability of NNS model, the computational accuracy of DNNS method are enhanced. The DNNS modeling is illustrated as follows:

Within a certain time domain [0, T], for the j-th input random variable $\boldsymbol{x}_j(t)$ ($\boldsymbol{x}_j(t) \in \boldsymbol{R}^n$) of assessment system, the corresponding output response is assumed as $Y_j[\boldsymbol{x}_j(t)]$ ($Y_j[\boldsymbol{x}_j(t)] \in \boldsymbol{R}$). On account of extremum selection mechanism in Fig. 1, the maximum response $Y_{j,\max}[\boldsymbol{x}_j(t)]$ of output responses series is indicated as

$$\boldsymbol{Y}_{j,\max}\left[\boldsymbol{x}_j(t)\right] = \mathrm{Max}_j\left\{Y_j\left[\boldsymbol{x}_j(t)\right] : j = 1, 2, \cdots, l\right\} \quad (1)$$

Considering the j-th generated samples $\{\boldsymbol{x}_j(t), Y_{j,\max}[\boldsymbol{x}_j(t)]\}$, the output response curve $Y(\boldsymbol{x})$ of assessment system can be fitted by a nonlinear fitting function $f(\boldsymbol{x})$, which maps a point in the space $\boldsymbol{R}^n$ onto the space $\boldsymbol{R}$

$$Y(\boldsymbol{x}) = f(\boldsymbol{x}) = \left\{\boldsymbol{x}_j(t) \xrightarrow[nonlinear\ fit]{\boldsymbol{R}^n \to \boldsymbol{R}} \boldsymbol{Y}_{j,\max}\left(\boldsymbol{x}_j(t)\right)\right\} \quad (2)$$

Nonlinear fitting function $f(\boldsymbol{x})$ is a key factor to gain valid mapping relationships between input random variables and output maximum response, since a good-performance $f(\boldsymbol{x})$ is beneficial to enhance computing efficiency and accuracy. In this case, for the certain input random variables $\boldsymbol{x}(t)$ and output maximum response $Y_{\max}[\boldsymbol{x}(t)]$, a dynamic neural network surrogate as shown in Fig. 2 with time-varying processing ability and related error control technique is adopted as

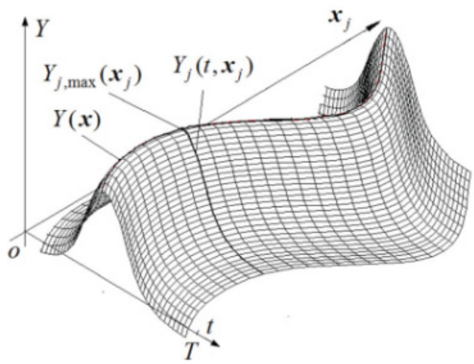

FIGURE 1. Extremum response mechanism.

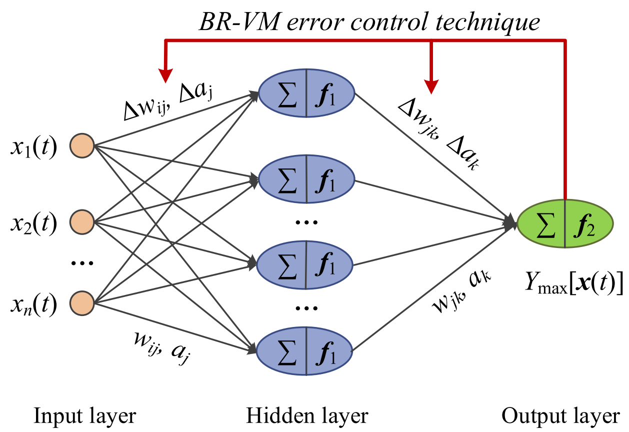

FIGURE 2. DNNS modeling.

the nonlinear fitting function, i.e.,

$$f(\boldsymbol{x}) = f_2\left[\sum_{j=1}^{l} \boldsymbol{\omega}_{jk} f_1\left(\sum_{i=1}^{n} \boldsymbol{\omega}_{ij}\boldsymbol{x}_i(t) + \boldsymbol{a}_j\right) + \boldsymbol{a}_k\right] \quad (3)$$

where $f_1(\cdot), f_2(\cdot)$ represents the 'tansig' and 'purelin' inspirit functions in hidden layer and output layer, respectively; $\boldsymbol{\omega}_{jk}$ the connection weight between the j-th neuron in input layer and the k-th neuron in hidden layer; $\boldsymbol{\omega}_{ij}$ the connection weight between the i-th neuron in hidden layer and the j-th neuron in output layer; $\boldsymbol{a}_j$ the j-th activation threshold of hidden layer; $\boldsymbol{a}_k$ the k-th activation threshold of the output layer; n, l the neuron number of input layer and hidden layer, respectively.

The effectiveness of the aforementioned DNNS model largely depends on the undetermined parameters, i.e., connection weights $\boldsymbol{\omega}$ and activation thresholds $\boldsymbol{a}$. Once the optimal undetermined parameters are obtained, the unbiased regression of output maximum response is acquired, and thereby the high-fidelity assessment is ensured. Therefore, the problem of dynamic surrogate modeling is transformed to find the optimal solution $\boldsymbol{\zeta}^*$

$$\boldsymbol{\zeta}^* = \arg\min_{\zeta} E(\boldsymbol{x}, \boldsymbol{\zeta}) \quad (4)$$

where $\boldsymbol{\zeta} = \{\boldsymbol{\omega}, \boldsymbol{a}\}$ indicates the vector representation of undetermined parameters; $E(\cdot)$ the training cost function.

For obtaining the optimal undermined parameters $\boldsymbol{\zeta}^*$ and enhancing the approximation performance of DNNS model, we present a BR-VM error control technique, which adopts Bayesian regularization (BR) theory to design training cost function for avoiding overfitting problems and variable metric (VM) algorithm to acquire the optimal undetermined parameters for preventing premature convergence.

To train for the optimal undetermined parameters and evaluate the generalization accuracy of fitted DNNS model, it is vital to design suitable training cost function to provide appropriate direction information in training process. In general, the training cost function $E_p(\boldsymbol{\zeta})$ in surrogate modeling is indicated as

$$E_P(\boldsymbol{\zeta}) = \|e(\boldsymbol{\zeta})\|_2^2 \quad (5)$$

where $e(\cdot)$ is training error function; $||\cdot||_2$ 2-norm function.

Supposing that the undetermined parameters $\boldsymbol{\zeta}$ in k-th iteration is $\boldsymbol{\zeta}^k$ and it changes little between two iterations, the training error function $e(\boldsymbol{\zeta})$ can be approximately evaluated at $\boldsymbol{\zeta}^k$ position by Taylor series expansion, then the training cost function $E_p(\boldsymbol{\zeta})$ is converted into

$$E_P(\boldsymbol{\zeta}) \approx \left\| e\left(\left(\boldsymbol{\zeta}^{(k)}\right) + J\left(\boldsymbol{\zeta}^{(k)}\right)\left(\boldsymbol{\zeta}^{(k+1)} - \boldsymbol{\zeta}^{(k)}\right)\right)\right\|_2^2 \quad (6)$$

where $J(\cdot)$ denotes the Jacobian matrix; $\boldsymbol{\zeta}^{(k+1)}$ the undetermined parameters $\boldsymbol{\zeta}$ in $(k+1)$-th iteration.

In fact, considering the training data often contain noise information, the overfitting problems would happen if directly using the above training cost function. In this case, it is inevitable to increase modeling complexity and degrade the generalization performance of the fitted DNNS model. To address this problem, we redesign the training cost function by employing BR theory, which can reduce the data-noise influence by decreasing feature dimension of input variables [44]. With minor values of undetermined parameters, the network structure of DNNS model is converting much simpler, and the overfitting problems are also pledged to be avoided. To perform the BR-based training cost function design, we first introduce the BR function $E_I(\boldsymbol{\zeta})$ as

$$E_I(\boldsymbol{\zeta}) = \begin{cases} E_L(\boldsymbol{\zeta}) = \sum_{l=1}^{L}\left(\left|\boldsymbol{\zeta}^{(k)}\right|\right), & \text{Lasso scheme} \\ E_R(\boldsymbol{\zeta}) = \left\|\sum_{r=1}^{R}\left(\boldsymbol{\zeta}^{(k)}\right)\right\|_2^2, & \text{Ridge scheme} \end{cases} \quad (7)$$

where $E_L(\boldsymbol{\zeta})$, $E_R(\boldsymbol{\zeta})$ represent the BR functions obtained by Lasso and Ridge schemes, respectively.

Compared with Lasso scheme reducing the majority of variable features to 0, Ridge scheme only decreases the minority of irrelevant variable features to 0 while the relevant variable features are still included. Considering that the Ridge scheme can describe more variable features than Lasso scheme, we adopt the Ridge scheme to creep-fatigue reliability assessment problem, because the output response of reliable creep-fatigue life is influencing by various input variables such as material properties, physical loads, model parameters, etc. Therefore, the BR-based training cost function E_{BR} is introduced as

$$\begin{aligned} E_{BR}(\boldsymbol{\zeta}) &= \alpha E_P(\boldsymbol{\zeta}) + \beta E_R(\boldsymbol{\zeta}) \\ \text{s.t. } E_R(\boldsymbol{\zeta}) &= \left\| \sum_{r=1}^{R} \left(\boldsymbol{\zeta}^{(k)}\right) \right\|_2^2 \end{aligned} \tag{8}$$

where α, β indicate the regularization factors, which are used to balance the training objective of fitting accuracy and the reduction objective of model complexity.

According to Eq. (6), the BR-based training cost function E_{BR} is rewritten as

$$\begin{aligned} E_{BR}(\boldsymbol{\zeta}) = \alpha \left\| e\left(\left(\boldsymbol{\zeta}^{(k)}\right) + J\left(\boldsymbol{\zeta}^{(k)}\right)\left(\boldsymbol{\zeta}^{(k+1)} - \boldsymbol{\zeta}^{(k)}\right)\right) \right\|_2^2 \\ + \beta \left\| \sum_{r=1}^{R} \left(\boldsymbol{\zeta}^{(k)}\right) \right\|_2^2 \end{aligned} \tag{9}$$

To efficiently resolve the nonlinear optimal problem in Eq. (4) and obtain the precise undetermined parameters of DNNS model, an optimal searching algorithm with high-speed and good-convergence virtues is necessarily required. As a super-linear convergence algorithm, VM algorithm possesses fast searching rate and high convergent accuracy in nonlinear optimization problems [46]. Therefore, in this study, the VM algorithm is adopted to find the optimal parameters of DNNS model. The basic thought of VM algorithm is to reduce the operating tasks and executive complexity by approximating positive definite matrix rather than the complicated Hessian matrix inversion. In this case, we first introduce the metric matrix of VM algorithm as

$$\nabla^2 E_{BR}(\boldsymbol{\zeta}^{(k+1)}) \approx \frac{\boldsymbol{\zeta}^{(k+1)} - \boldsymbol{\zeta}^{(k)}}{\nabla E_{BR}\left(\boldsymbol{\zeta}^{(k+1)}\right) - \nabla E_{BR}\left(\boldsymbol{\zeta}^{(k)}\right)} \tag{10}$$

Supposing that $\mu^{(k)} = \boldsymbol{\zeta}^{(k+1)} - \boldsymbol{\zeta}^{(k)}$, $\nu^{(k)} = \nabla E_{BR}(\boldsymbol{\zeta}^{(k+1)}) - \nabla E_{BR}(\boldsymbol{\zeta}^{(k)})$ and Hessian matrix $\boldsymbol{H}^{(k+1)} = \nabla^2 E_{BR}(\boldsymbol{\zeta}^{(k+1)})$, then the $(k+1)$-th metric $\boldsymbol{H}^{(k+1)}$ can be obtained by DFP formula [47], i.e.,

$$\begin{aligned} \boldsymbol{H}^{(k+1)} = \boldsymbol{H}^{(k)} + \frac{\boldsymbol{\mu}^{(k)}\boldsymbol{\mu}^{(k)T}}{\boldsymbol{\mu}^{(k)T}\boldsymbol{\nu}^{(k)}} - \frac{\boldsymbol{\mu}^{(k)}\boldsymbol{\nu}^{(k)T}\boldsymbol{H}^{(k)}}{\boldsymbol{\mu}^{(k)T}\boldsymbol{\nu}^{(k)}} \\ - \frac{\boldsymbol{H}^{(k)}\boldsymbol{\nu}^{(k)}\boldsymbol{\mu}^{(k)T}}{\boldsymbol{\mu}^{(k)T}\boldsymbol{\nu}^{(k)}} \end{aligned} \tag{11}$$

For a given searching direction $\boldsymbol{d}^{(k)}$ and step length $\delta^{(k)}$, the updating formula of VM algorithm can be deduced as

$$\begin{aligned} \boldsymbol{\zeta}^{(k+1)} &= \boldsymbol{\zeta}^{(k)} + \boldsymbol{d}^{(k)}\boldsymbol{\delta}^{(k)} \\ \text{s.t. } \boldsymbol{d}^{(k)} &= -\boldsymbol{H}^{(k+1)}\nabla E_{BR}\left(\boldsymbol{\zeta}^{(k)}\right) \end{aligned} \tag{12}$$

In VM updating process, optimal step length $\delta^{(\mathrm{k})}$ in each iteration should be acquired to guarantee the continual decrease of training cost function $E_{BR}(\eta)$. In this case, it results from Armijo-Goldstein criteria and strong Wolfe

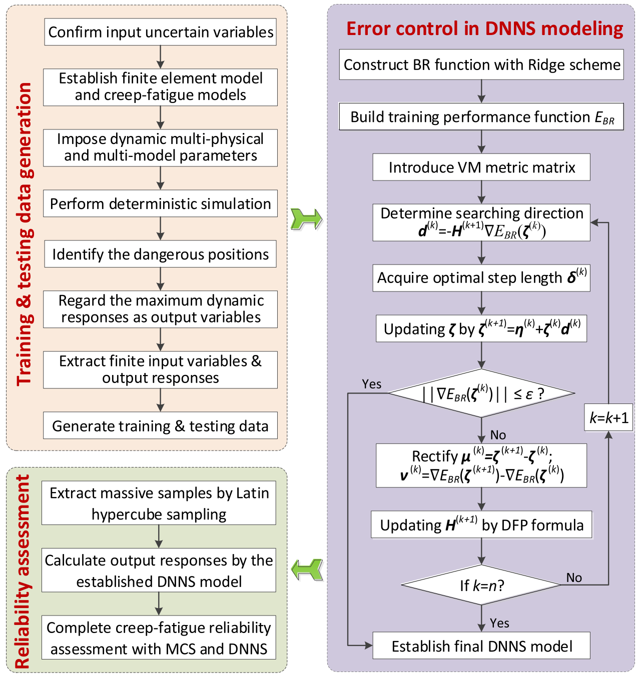

FIGURE 3. Flow chart of reliability assessment with DNNS modeling.

non-exact line searching [50], we further introduce the iteration formula of optimal step length $\delta^{(k)}$ as

$$\begin{cases} E_{BR}\left(\boldsymbol{\zeta}^{(k+1)}\right) \le E_{BR}\left(\boldsymbol{\zeta}^{(k)}\right) + \xi\boldsymbol{\delta}^{(k)}\nabla E_{BR}\left(\boldsymbol{\zeta}^{(k)}\right)^T \boldsymbol{d}^{(k)} \\ \varsigma \left| \nabla E_{BR}\left(\boldsymbol{\zeta}^{(k)}\right)^T \boldsymbol{d}^{(k)} \right| \le \left| \nabla E_{BR}\left(\boldsymbol{\zeta}^{(k)}\, \boldsymbol{C}\, \boldsymbol{\delta}^{(k)}\boldsymbol{d}^{(k)}\right)^T \boldsymbol{d}^{(k)} \right| \end{cases} \tag{13}$$

in which control factor $\xi \in (0, 0.5)$, $\varsigma \in (\xi, 1)$.

By performing the VM algorithm, the undetermined parameters $\boldsymbol{\zeta}^*$ can be acquired, and the DNNS model is established consequently. Noticeably, the presented BR-VM error control technique is conducive to reduce the computing complexity and enhance the approximating accuracy of DNNS model. By fusing the BR-VM error control technique into DNNS modeling, the flow chart of reliability assessment is summarized in Fig. 3.

B. MULTI-SURROGATE COLLABORATION APPROACH

In this subsection, multi-surrogate collaboration approach (MSCA) is developed by absorbing the strength of DNNS model into distributed collaborative strategy. We will study the MSCA including basic theory and mathematical model.

Creep-fatigue reliability assessment refers to multi-level issues (i.e., stress/strain prediction level and creep-fatigue life assessment level, etc.), which brings in time-wasting simulation tasks and huge computing complexity in program execution. Aim at the multi-level problems, the distributed collaborative strategy was developed by Song and Bai to enhance the computing efficiency and accuracy. In multi-failure probabilistic analysis and low cycle fatigue life prediction, the strategy had been validated to hold fast speed and acceptable precision [48], [49]. Along with the heuristic strategy, we develop a multi-surrogate collaboration approach with respect to the DNNS model and distributed collaborative strategy, to address the strong-nonlinearity and high-complexity issues and enhance computing efficiency in creep-fatigue reliability assessment. The basic thought of MSCA is summarized as:

(1) Distribute the entire complex multi-level model into several simple single-level models (sub-models) in respect of the prediction layers and response traits. And each sub-model is dependent each other.

(2) Realize the deterministic analyses with consideration of multi-physical parameters and multi-model parameters, to determine the creep-fatigue position as sampling location.

(3) Draw finite input variable & output response samples by adopting Latin hypercube sampling technique and FE simulations. The sample set is regarded as training & testing data for DNNS modeling.

(4) Build distributed DNNS models by the training & testing data and the BR-VM error control technique. With performing distributed DNNS simulations, the statistical traits of distributed output responses are obtained.

(5) Regard the distributed output responses and multi-model parameters as input variables, creep-fatigue life as output response, the collaborative DNNS model is built.

(6) Retrieve the distribution characteristics of creep-fatigue life by executing the collaborative DNNS simulations.

Accompanying with the heuristic distributed process and collaborative process, the presented MSCA divides the whole complex multi-level surrogate modeling into the several simple multi-level sub-modeling, which is conducive to reduce the nonlinearity of reliability assessment and thus brings convenience for enhancing efficiency and accuracy.

Supposing that the reliability assessment system involves h levels, the complicated multi-level problem is converted to a series of simple single-level problems by employing the distributed collaborative strategy, the input samples of the p-th level $\boldsymbol{x}^{(p)}$ and the corresponding output response $\boldsymbol{Y}^{(p)}$ is

$$\begin{cases} \boldsymbol{Y}^{(p)} = f\left(\boldsymbol{x}^{(p)}\right) p = 1, 2, \cdots, h \\ \boldsymbol{x}^{(p)} = \left[x_1^{(p)}, x_2^{(p)}, \cdots, x_n^{(p)}\right]^{\mathrm{T}} \end{cases} \tag{14}$$

According to the developed DNNS model shown in Eq. (3), the distributed DNNS model under the p-th level is

$$\tilde{Y}^{(p)} = f_2\left[\sum_{j=1}^{l} \tilde{\omega}_{jk}^{(p)} f_1\left(\sum_{i=1}^{n} \tilde{\omega}_{ij}^{(p)} \boldsymbol{x}_i^{(p)}(t) + \tilde{a}_j^{(p)}\right) + \tilde{a}_k^{(p)}\right] \tag{15}$$

where $\tilde{\boldsymbol{\omega}}_{jk}^{(p)}$, $\tilde{\boldsymbol{\omega}}_{ij}^{(p)}$, $\tilde{\boldsymbol{a}}_j^{(p)}$ and $\tilde{\boldsymbol{a}}_k^{(p)}$ are optimal solutions of training function in the p-th distributed DNNS model.

Because of the distributed output responses $\{\tilde{\boldsymbol{Y}}^{(p)}\}hp = 1$ as input variables $\tilde{\boldsymbol{x}}$, the collaborative DNNS model with multiple levels is deduced as

$$\begin{cases} \tilde{\boldsymbol{Y}} = f_2\left[\sum_{j=1}^{l} \tilde{\boldsymbol{\omega}}_{jk} f_1\left(\sum_{i=1}^{n} \tilde{\boldsymbol{\omega}}_{ij} \tilde{\boldsymbol{x}}_i(t) + \tilde{\boldsymbol{a}}_j\right) + \tilde{\boldsymbol{a}}_k\right] \\ \tilde{\boldsymbol{x}} = \left\{\tilde{\boldsymbol{Y}}^{(p)}\right\} p = 1, 2, \cdots, h \end{cases} \tag{16}$$

where $\tilde{\boldsymbol{\omega}}_{jk}$, $\tilde{\boldsymbol{\omega}}_{ij}$, $\tilde{\boldsymbol{a}}_j$ and $\tilde{\boldsymbol{a}}_k$ are optimal solutions of training function of the collaborative DNNS model.

From the above analysis, the DNNS (Eq. (3)) model with many levels is divided into a series of distributed DNNS sub-models (Eqs. (14)-(15)) and one collaborative DNNS sub-model (Eq. (16)). We call the DNNS modeling with distributed collaborative strategy as multi-surrogate collaboration approach, which is suitable for complex multi-level reliability assessment problems.

C. CREEP-FATIGUE RELIABILITY ASSESSMENT THEORY

In this subsection, the creep-fatigue reliability assessment theory is presented by employing the proposed MSCA. We will investigate the creep-fatigue reliability assessment including creep-fatigue reliable life prediction and the related parameter sensitivity analysis.

Creep-fatigue reliability assessment is to evaluate the overall creep-fatigue reliability index of complex structure and to identify the influencing extent of uncertain parameters on structural safety. In single-level distributed analysis, assuming that the allowable response on in p-th level is $[Y^{(p)}]$, the p-th distributed limit state function $g^{(p)}(\boldsymbol{x})$ based on the p-th distributed DNNS is

$$g^{(p)}(\boldsymbol{x}) = \left[Y^{(p)}\right] - f_2\left[\sum_{j=1}^{l} \tilde{\boldsymbol{\omega}}_{jk}^{(p)} f_1\left(\sum_{i=1}^{n} \tilde{\boldsymbol{\omega}}_{ij}^{(p)} \boldsymbol{x}_i^{(p)}(t) + \tilde{\boldsymbol{a}}_j^{(p)}\right) + \tilde{\boldsymbol{a}}_k^{(p)}\right] \tag{17}$$

To screen insignificant information and rank the importance of uncertain parameters, the distributed sensitivity analysis by describing the variables influence degree on the failure probability. For variables with higher sensitivity degree, changes in their distribution parameters will lead to a greater change in the failure probability, and vice versa. With massive input variables and output responses in p-th level, the distributed sensitivity degrees of input variables on failure probability are developed by

$$\begin{gathered} S^{(p)} = \mu\left(\frac{L_f\left[g^{(p)}(\boldsymbol{x}_l)\right]\left(\boldsymbol{x}_{ij}^{(p)} - \mu\left(\boldsymbol{x}_i^{(p)}\right)\right)}{\nu\left(\boldsymbol{x}_i^{(p)}\right)}\right) \\ \text{s.t. } L_f\left[g^{(p)}(\boldsymbol{x}_l)\right] = \begin{cases} 1, & g^{(p)}(\boldsymbol{x}_l) \le 0 \\ 0, & g^{(p)}(\boldsymbol{x}_l) > 0 \end{cases} \end{gathered} \tag{18}$$

where $x_{il}^{(p)}$ is the i-th input vector of l-th data set under p-th level; $L_f[g^{(p)}(\boldsymbol{x}_l)]$ the logic function of failure domain under p-th layer; $\mu(\cdot)$ the mean value function; $\nu(\cdot)$ the variance value function. Note that input variables with higher sensitivity will pose larger impacts on failure probability, and vice versa.

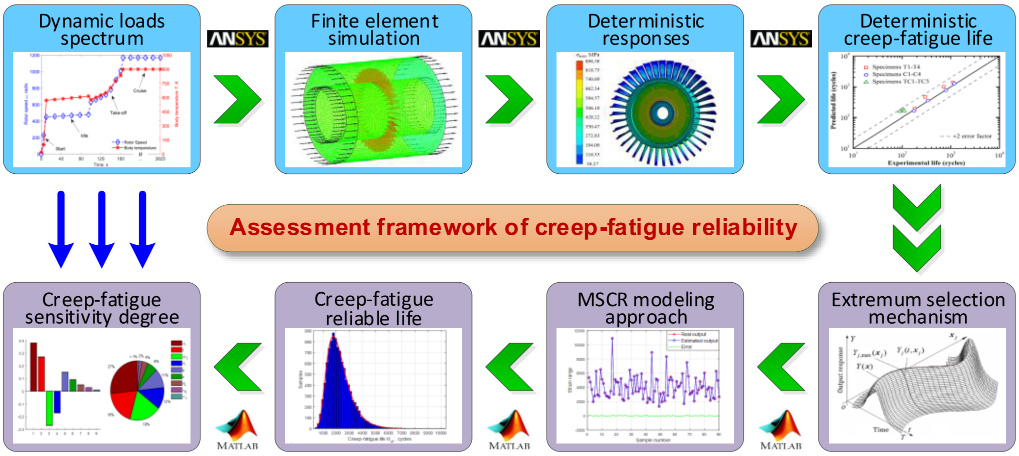

FIGURE 4. **Assessment framework of creep-fatigue reliability.**

In the multi-level collaborative analysis, the allowable output structural response is presuming as $[Y]$, then the collaborative limit state function based on the collaborative DNNS is obtained as

$$g\left(\boldsymbol{x}\right) = [Y] - f_2\left[\sum_{j=1}^{l} \tilde{\boldsymbol{\omega}}_{jk} f_1\left(\sum_{i=1}^{n} \tilde{\boldsymbol{\omega}}_{ij}\tilde{\boldsymbol{x}}_i\left(t\right) + \tilde{\boldsymbol{a}}_j\right) + \tilde{\boldsymbol{a}}_k\right] \tag{19}$$

Similarly, based on overall input variables and output responses, the collaborative sensitivity degrees of input variables on failure probability are introduced as

$$\begin{aligned} S &= \mu\left(\frac{L_f\left[g\left(\boldsymbol{x}_l\right)\right]\left(\boldsymbol{x}_{il} - \mu\left(\boldsymbol{x}_i\right)\right)}{\nu\left(\boldsymbol{x}_i\right)}\right) \\ \text{s.t. } L_f\left[g\left(\boldsymbol{x}_l\right)\right] &= \begin{cases} 1, & g\left(\boldsymbol{x}_l\right) \leq 0 \\ 0, & g\left(\boldsymbol{x}_l\right) > 0 \end{cases} \end{aligned} \tag{20}$$

Based on the collaborative DNNS model and the above simulated samples in sensitivity analysis, the structural creep-fatigue reliability is calculated as

$$\begin{aligned} R &= \frac{1}{N}\sum_{i=1}^{N} L_r\left[g\left(\boldsymbol{x}_l\right)\right] = \frac{N_r}{N} \\ \text{s.t. } L_r\left[g\left(\boldsymbol{x}_l\right)\right] &= \begin{cases} 1, & g\left(\boldsymbol{x}_l\right) \leq 0 \\ 0, & g\left(\boldsymbol{x}_l\right) > 0 \end{cases} \end{aligned} \tag{21}$$

where $L_r[g(\boldsymbol{x}_l)]$ is the logic function of whole secure domain, it either to be 1 when $g(\boldsymbol{x}_l) \geq 0$, or to be 0 when $g(\boldsymbol{x}_l) < 0$; N_r, N the number of secure and total points, respectively.

According to creep-fatigue reliability assessment theory, the complex creep-fatigue reliability assessment is split into a series of distributed analyses and a collaborative analysis, the efficiency of creep-fatigue reliability assessment is promising to be enhanced by alleviating the simulation burdens in each analysis and conducting automatic parallel calculations on several devices. The assessment framework of creep-fatigue reliability with the presented MSCA is drawn in Fig. 4.

III. CREEP-FATIGUE RELIABILITY ANALYSIS OF TURBINE ROTOR

In the extreme service environment of high thermal gradient, large gas pressure and strong centrifugal force, turbine rotor endure huge tensile stress and creep-fatigue damage. Moreover, the material variability, load fluctuation and model uncertainty bring about large discreteness for turbine rotor creep-fatigue life. In this study, to predict creep-fatigue life and evaluate reliability performance of turbine rotor and even whole-body aircraft engine, the creep-fatigue reliability analysis was discussed by using the presented MSCA. It should be noted that all computations are performed on an Inter(R) Core(TM) Desktop Computer (i7-9700K CPU 3.6 GHz and 16 GB RAM).

A. MATERIAL PREPARATIONS

A typical turbine rotor in aircraft engine is displayed in Fig. 5. Because of the high temperature and high velocity gas from main chamber combustion and high rotor centrifugal force from inertia force field, by regarding the upper edge of turbine disk as inside wall, the inner surface of turbine casing as outside wall, and the turbine blade surface as multi-physical interaction (MPI) surface, we establish the multi-physical FE model with consideration of the nonlinear interaction effects of fluid field, thermal field and structural field. The multi-physical FE model [48] of turbine rotor is shown in Fig. 6. Considering the multi-physical loads of turbine rotor are constantly changing in flight mission cycle, we consider the body temperature and rotor speed as time-varying loads in this study. The time-varying loads spectrum [35] of turbine rotor are displayed in Fig. 7.

To quantify the random uncertainties of material properties and time-varying loads, the multi-physical parameters (i.e., rotor speed ω, body temperature T, gas velocity v, material density ρ, thermal transfer coefficient h and thermal expansion coefficient κ) are regarded as the multi-physical random variables. The distribution characteristics of multi-physical

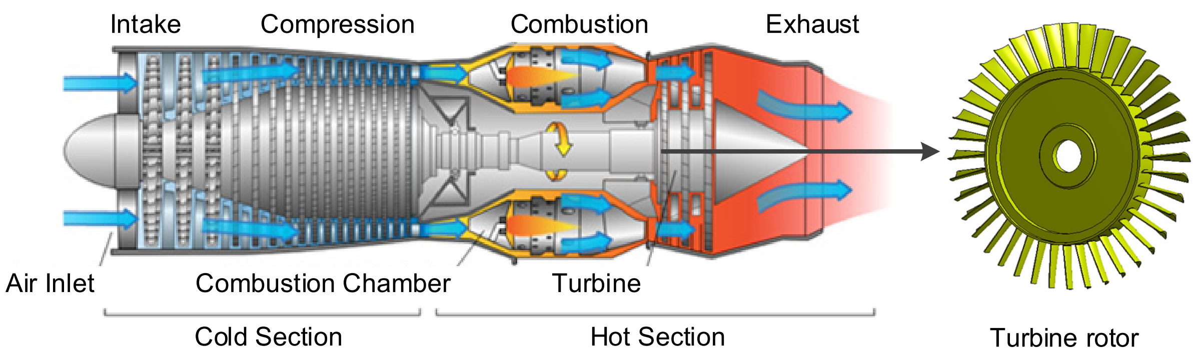

FIGURE 5. Sketch of turbine rotor.

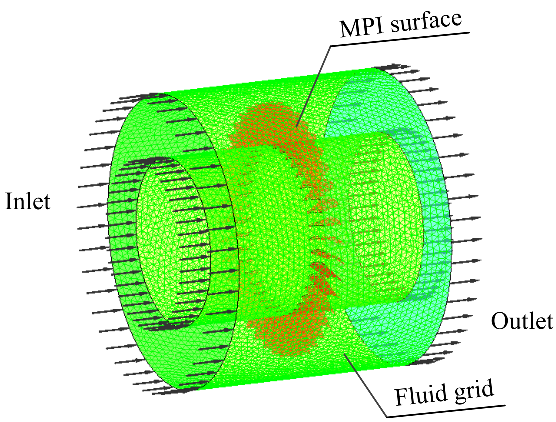

FIGURE 6. The MPI sketch of turbine rotor.

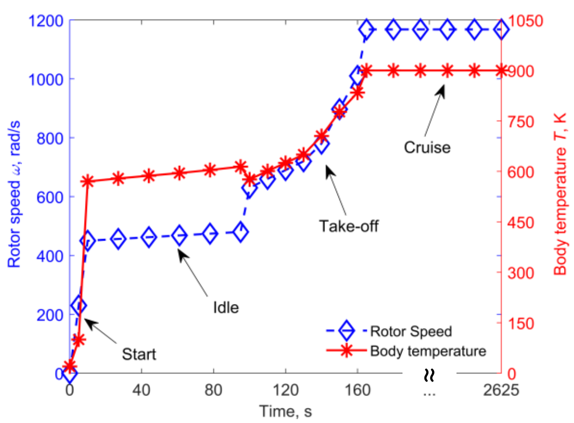

FIGURE 7. Time-varying loads spectrum of turbine rotor.

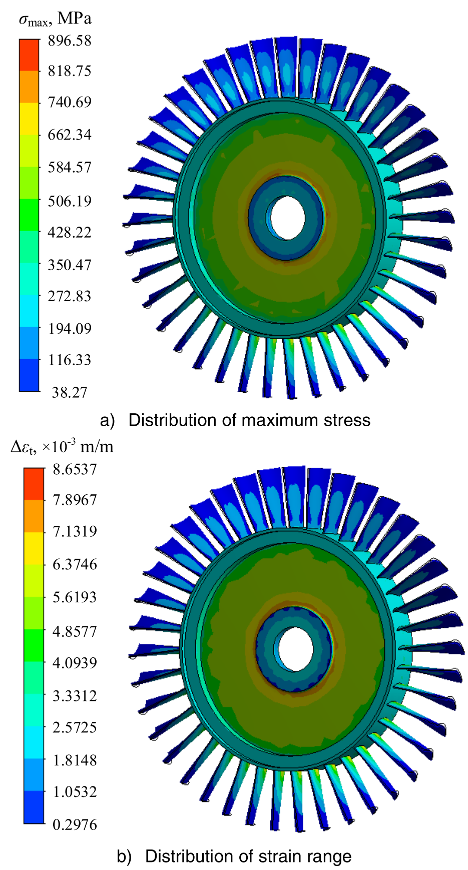

FIGURE 8. Distributions of maximum stress and strain range.

parameters are shown in Table 1. Likewise, to measure the random uncertainties of creep-fatigue life models involve Masson-Coffin fatigue model [51], Larson-Miller creep model [52] and Mao's creep-fatigue model [53], [54], the multi-model parameters (i.e., fatigue strength exponent b, fatigue ductility exponent c, fatigue strength coefficient σ'_{f}, fatigue ductility coefficient $\varepsilon'_{\mathrm{f}}$, the holding creep time t, and the creep-fatigue parameter θ_1 and creep-fatigue parameter θ_2) are considered as the multi-model random variables. The distribution characteristics of multi-model parameters are listed in Table 2. Note that the fatigue ductility coefficient $\varepsilon'_{\mathrm{f}}$ obeys lognormal distribution and other random variables obey normal distribution, all of selected random variables are reciprocally independent.

B. DETERMINISTIC ANALYSES

With importing the mean values of multi-physical parameters from Table 1 into the FE model, the multi-physical FE simulation analysis is performed with respect to the

TABLE 1. Distribution characteristics of multi-physical parameters.

Variables	ω, rad·s^{-1}	T, K	v, m/s	ρ, 10^{-9} t·mm^{-3}	h, W·m^{-2}·K^{-1}	κ, 10^{-6}℃
Mean	1168	1 150	168	8.21	11756	14.16
Variance	23.36	15.56	3.2	0.164	235.12	0.2832
Distribution	Normal	Normal	Normal	Normal	Normal	Normal

TABLE 2. Distribution characteristics of multi-model parameters.

Variables	t, s	θ_1	θ_2	b	c	σ_f', MPa	ε_f'
Mean	2460	0.7356	-9.066	-0.1	-0.84	1419	0.505
Variance	49.2	0.01473	0.1813	0.002	0.0168	28.38	0.0101
Distribution	Normal	Normal	Normal	Normal	Normal	Normal	Lognormal

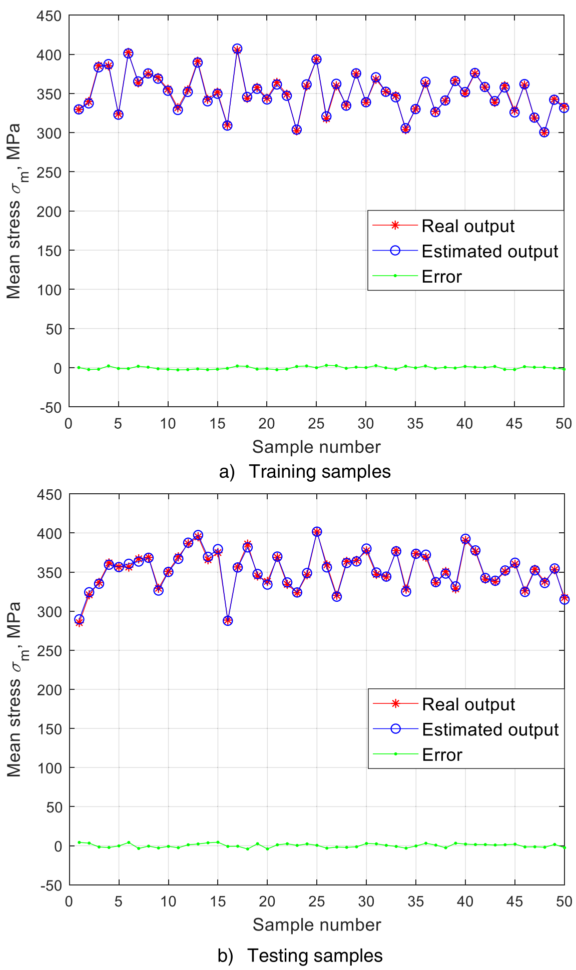

FIGURE 9. Prediction result of distributed DNNS-1 model.

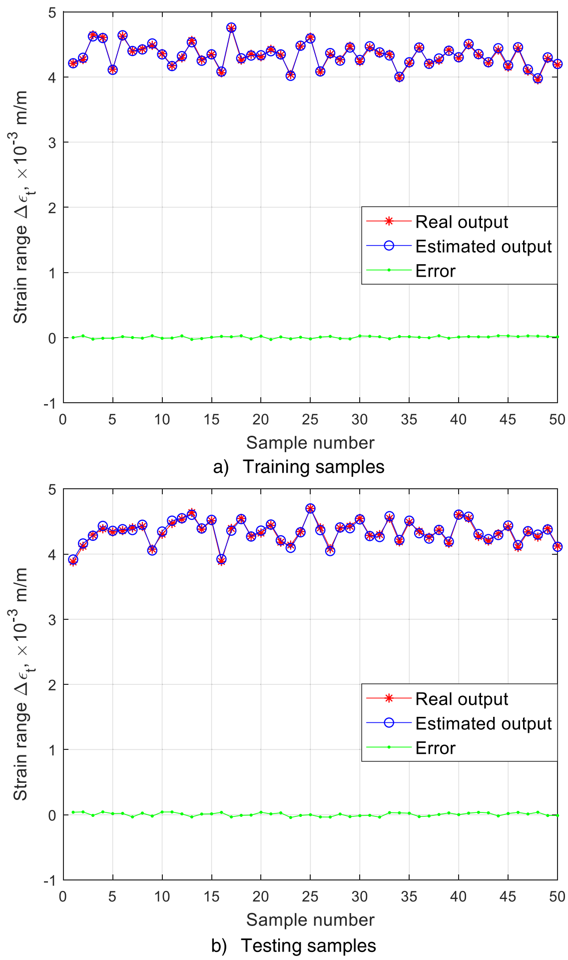

FIGURE 10. Prediction result of distributed DNNS-2 model.

multi-physical coupling effects of fluid loads, thermal loads and structural loads. According to the large deformation theory and stress/strain constitutive relationship, the deterministic stress-strain responses (i.e., maximum stress σ_{max} and strain range $\Delta\varepsilon_t$) of turbine rotor are obtained as drawn in Fig. 8. From the multi-physical FE simulation, we observe that the creep-fatigue damage appears at the blade root site in back surface. Hence, the responses in blade root site are selected as the output responses to perform the subsequent creep-fatigue assessments. According to the max-stress cycle 0-σ_{max}-0, the mean stress σ_m and strain range $\Delta\varepsilon_t$ of blade root site are obtained as 352.49 MPa and 4.32×10^{-3} m/m, respectively.

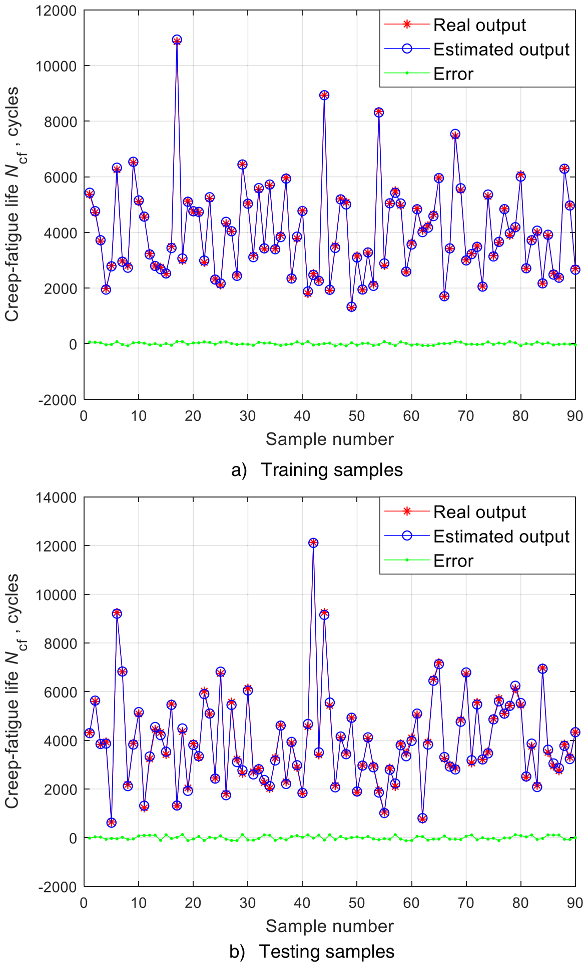

FIGURE 11. Prediction result of collaborative DNNS model.

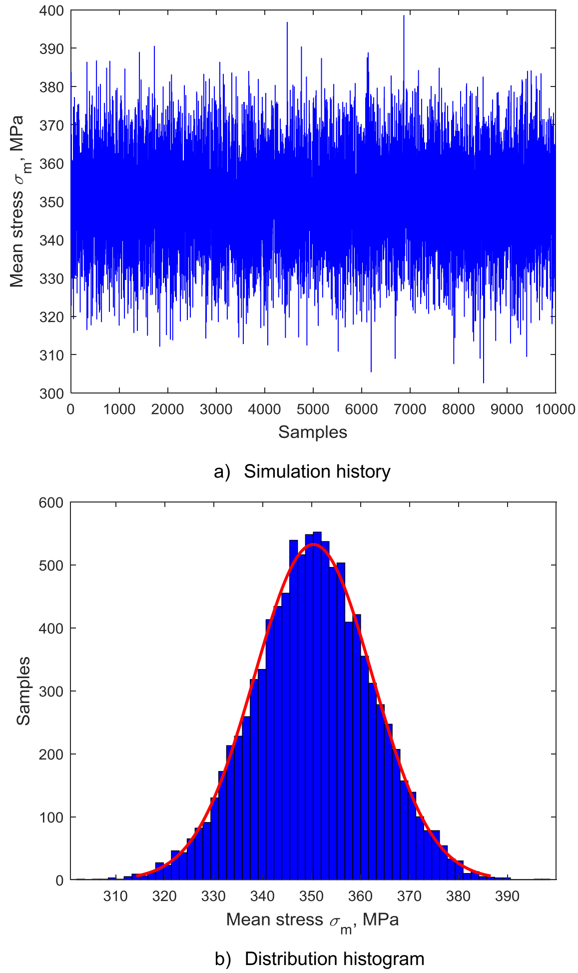

FIGURE 12. Mean stress curve of turbine rotor.

Similarly, with inputting the mean values of multi-model parameters from Table 2 into the creep-fatigue prediction models (i.e., Masson-Coffin model, Larson-Miller model and Mao's creep-fatigue model), the creep-fatigue life analysis is executed with regard to the interaction effects of fatigue damage and creep damage, the deterministic creep-fatigue life of the turbine rotor is obtained as 1386 cycles. Note that the computing device has took 203 seconds to perform one-time multi-physical FE simulation, which is also illustrates that it is unaffordable to repeatedly simulate thousands of multi-physical FE simulations.

C. MSCA MODELING

To alleviate the computational burdens and enhance computing accuracy of creep-fatigue reliability assessment, we divide the 'big' creep-fatigue reliability assessment modeling with strong-nonlinearity and large-dynamicity into a 'simple' distributed stress/strain modeling and a 'simple' collaborative creep-fatigue modeling, by the presented MSCA modeling. The detailed modeling procedures are summarized as follows:

(1) Distributed stress/strain modeling: Based on the statistical characteristics of multi-physical parameters in Table 1, we extract 100 groups of input multi-physical parameters into FE simulation, the corresponding output responses of mean stress σ_m and strain range $\Delta\varepsilon_t$ are obtained. To establish the optimal DNNS model and validate its generalization performance, the 100 groups of multi-physical variables and stress/strain responses are equally divided into training samples and testing samples. Based on the proposed BR-VM training algorithm, the optimal distributed DNNS models for σ_m and $\Delta\varepsilon_t$ (termed as distributed DNNS-1 model and distributed DNNS-2 model) are constructed by training samples, and its generalization abilities are tested by testing samples. Through comparing the real outputs with these of training samples and testing samples, the prediction results of distributed DNNS-1 model and distributed DNNS-2 model are drawn in Figs. 9-10, respectively.

(2) Collaborative creep-fatigue modeling: based on the statistical characteristics of multi-model parameters in Table 2, we consider 180 groups of multi-model parameters and the simulated σ_m and $\Delta\varepsilon_t$ as input variables, the related creep-fatigue life N_{cf} can be retrieved by adopting creep-fatigue prediction models. Similarly, by dividing the 180 groups of multi-model variables and creep-fatigue life into two mutually exclusive samples set (i.e., training samples

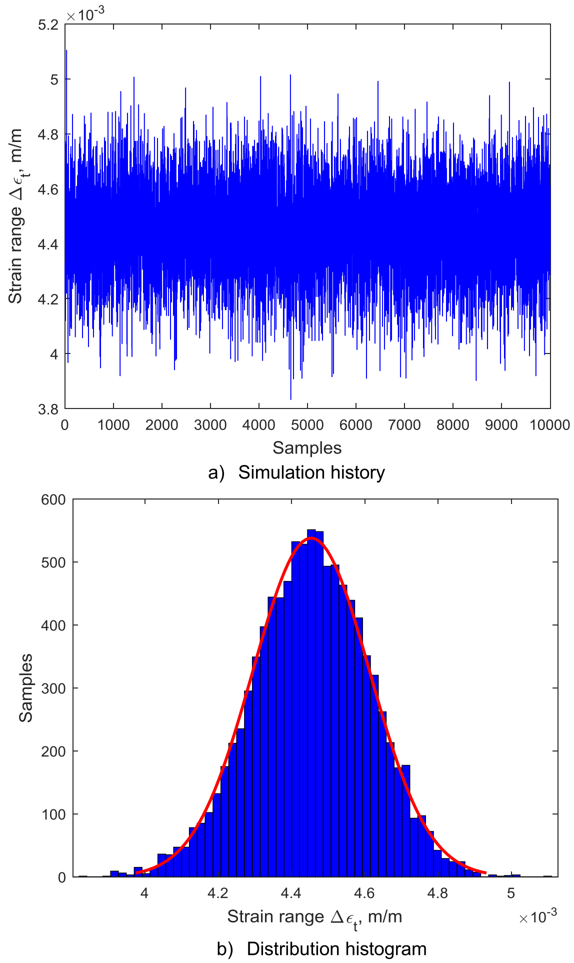

FIGURE 13. **Strain range curve of turbine rotor.**

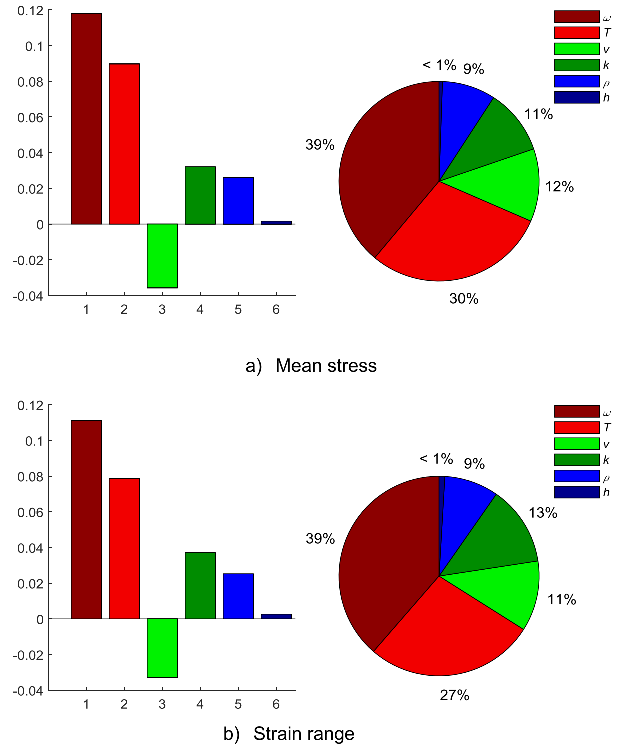

FIGURE 14. **Sensitivities and effect probabilities on stress/strain.**

and testing samples), the optimal collaborative DNNS model for N_{cf} is established by training samples and validated by testing samples. With comparing the real outputs with these of training samples and testing samples, the prediction results of collaborative DNNS is drawn in Fig. 11.

As shown in Figs. 9-11, we observe that even if the stress/strain responses and creep-fatigue life of turbine rotor possess large dispersion, the built MSCA models (i.e., distributed DNNS-1, distributed DNNS-2 and coordinated DNNS) still can fit each training & testing point with almost zero approximation or generalization errors. Therefore, based on the great approximation and generalization performances, the presented MSCA modeling is suitable to perform the creep-fatigue reliability analysis of turbine rotor.

D. CREEP-FATIGUE RELIABILITY ANALYSIS WITH MSCA

Based on the statistic traits of multi-physical parameters, we extract 10 000 groups of input variables by Latin hypercube sampling technique. By importing the input variables into the distributed DNNS models, the corresponding mean stress σ_m and strain range $\Delta\varepsilon_t$ responses are obtained, whose distribution histograms are depicted in Figs. 12-13. According to the stress/strain sensitivity analysis model in Eqs. (17-18) and the 10 000 groups of samples, we acquire the sensitivities and effect probabilities of input variables on stress/strain responses, which are illustrated in Fig. 14. Note that the sensitivities of input variables are signed where positive values indicate the positive correlation of output response with input variables, and vice versa.

As depicted in Figs. 12-13, the mean stress and strain range of turbine rotor nearly obey normal distributions. As revealed in Fig. 14, rotor speed and body temperature are the main influential factors on mean stress and strain range, the corresponding effecting probabilities of which are 39 %, 30 % for mean stress and 39 % and 27 % for strain range. Therefore, rotor speed and body temperature should be given priority in turbine rotor stress/strain design.

Based on the multi-model parameters in Table 2 and the simulated stress/strain responses as input variables, 10 000 collaborative DNNS simulations are executed to obtain the creep-fatigue life N_{cf}, whose distributing curve are drawn in Fig. 15. Based on the creep-fatigue sensitivity analysis model in Eqs. (19-20), the sensitivities and effect probabilities of all of input variables on creep-fatigue life are revealed in Fig. 16.

As illustrated in Fig. 15, with the given multi-physical and multi model parameters, the creep-fatigue life of the turbine rotor roughly obeys a lognormal distribution. Moreover, based on the creep-fatigue reliability model in Eq. (21), the creep-fatigue life of the turbine rotor under reliability 99.87 % is 629 cycles. Note that the assessed 629 cycles are suitable for the specified turbine rotor with material and loads

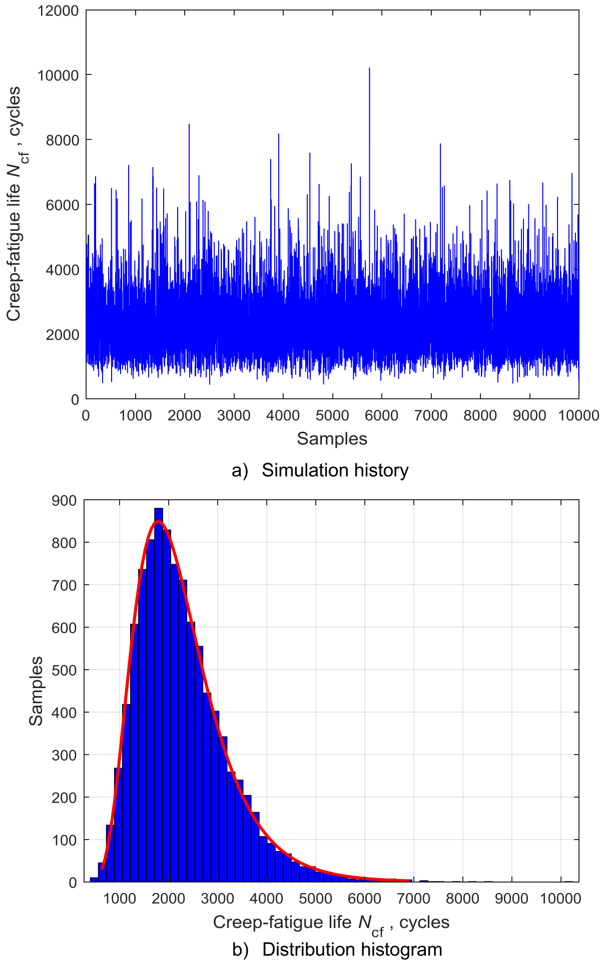

FIGURE 15. Creep-fatigue life curve of turbine rotor.

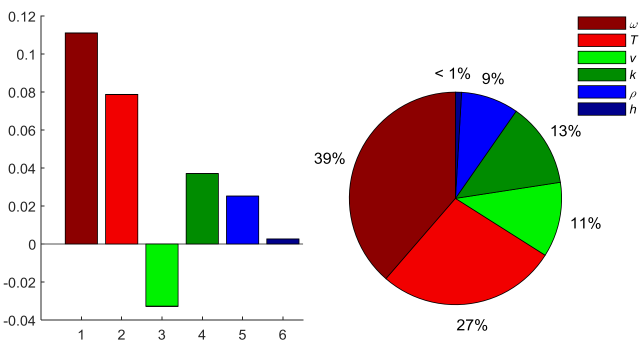

FIGURE 16. Sensitivities and effect probabilities on creep-fatigue life.

in Tables 1-2, and do not apply to all turbine rotors with different materials and loads. As shown in Fig. 16, for all of input variables on creep-fatigue life, the fatigue strength coefficient and the holding creep time plays a leading role on creep-fatigue life, which requires the highest attentions in the creep-fatigue design of turbine rotor.

E. METHOD VALIDATIONS

To validate the effectiveness of the proposed MSCA, the creep-fatigue reliability assessment of turbine rotor is also studied based on the direct Monte Carlo simulation (MCS), response surface (RS) method [32], neural network surrogate (NNS) method [6], and the presented DNNS method. Note that the simulation values obtained by the direct MCS are regarded as theoretical true values on account of the statistics theory and large-number law. To ensure the rationality of methods comparison, we have set the following ground rules: based on the same input parameters as shown in Tables 1-2, the creep-fatigue reliable life should be acquired. Note that the direct MCS, RS and NNS are directly executed in one computing device while the MSCA adopts the parallel computation of stress/strain response prediction and creep-fatigue life assessment. Moreover, before executing the creep-fatigue reliability assessment, the surrogate model methods (i.e., RS, NNS, DNNS and MSCA) would first perform the surrogate modeling with the required fitting number and fitting time. The computational efficiency and accuracy of different methods for creep-fatigue reliability assessment are listed in Tables 3-4, respectively.

As revealed in Table 3, the fitting number and fitting time of MSCA are less than RS, NNS and DNNS, and the simulation time of four surrogate model methods are far less than the direct MCS method. Moreover, the presented MSCA offers the highest computing efficiency and the superiorities becomes more obvious with increasing simulation times. The superior performance of MSCA is induced by a few vital factors: (i) the DNNS model-based MSCA only focuses on the extremum values rather than all of the dynamic responses within a time domain, and the high-efficiency surrogate modeling of DNNS models are rapidly accomplished by the proposed BR-VM error control technique; (ii) the distributed collaborative strategy-based MSCA accomplishes the distributed parallel computation by simulating surrogate models on multiple terminal devices simultaneously, which is conducive to reduce calculation complexity and enhance computational speed. Therefore, by integrating the DNNS proposed and distributed collaborative strategy, the MSCA can be established and employed in creep-fatigue reliability assessment with high computational efficiency.

As illustrated in Table 4, the presented MSCA possesses the highest computational accuracy than other surrogate model methods (RS, NNS and DNNS) and are almost consistent with the direct MCS method. The high computational accuracy and good generalization performance of MSCA result from the following issues: (i) the BR-VM error control technique-based MSCA avoids the overfitting problems and ensures accurate optimum searching, which contributes to enhance the nonlinear fitting ability and model generalization effects; (ii) the distributed collaborative strategy-based MSCA can dramatically reduce the nonlinearity of surrogate modeling, which is promising to guarantee the computing accuracy of creep-fatigue reliability assessment. Hence, by absorbing the virtues of BR-VM error control technique and distributed collaborative strategy, the proposed MSCA possesses high computational accuracy in creep-fatigue reliability assessment.

TABLE 3. Computational efficiency for creep-fatigue reliability assessment.

Methods	Fitting surrogate models		Computational time of different times, s				
	Fitting number	Fitting time, s	10^2	10^3	10^4	10^5	10^6
Direct MCS	–	–	1.97×10^4	3.52×10^5	4.63×10^6	5.86×10^7	–
RS	257	2.96×10^4	12.81	105.39	717.64	4.62×10^3	1.94×10^4
NNS	216	2.01×10^4	8.64	66.82	534.21	1.45×10^3	8.37×10^3
DNNS	185	1.75×10^4	5.48	21.53	162.52	983.67	6.21×10^3
MSCA	140	1.25×10^4	1.25	9.31	85.47	71.29	5.87×10^3

TABLE 4. Computational accuracy for creep-fatigue reliability assessment.

Methods	Creep-fatigue reliable life of different times, cycle					Computational accuracy of different times				
	10^2	10^3	10^4	10^5	10^6	10^2	10^3	10^4	10^5	10^6
Direct MCS	672	633	621	606	604	–	–	–	–	–
RS	759	716	685	668	651	0.8705	0.8765	0.8969	0.8977	0.9156
NNS	730	680	660	641	635	0.9137	0.9258	0.9372	0.9422	0.9486
DNNS	718	667	645	622	616	0.9315	0.9463	0.9614	0.9736	0.9801
MSCA	690	645	629	610	606	0.9732	0.9810	0.9871	0.9933	0.9967

Assuming that the N_{MCS} indicate the creep-fatigue reliable life obtained by direct MCS and N_{SM} denotes the creep-fatigue reliable life retrieved by surrogate models, the computational accuracy of each surrogate model is calculated by 1- [(|N_{MCS} - N_{MCS}|)/ N_{MCS}]×100 %

In summary, the proposed MSCA is proven to notably enhance the computational efficiency while keeping an acceptable computational accuracy, and hereby is a feasible and effective way for the creep-fatigue reliability assessment of turbine rotor.

IV. CONCLUSION

The objective of this study is to present a multi-surrogate collaboration approach (MSCA) based on dynamic neural network surrogate (DNNS) and distributed collaborative strategy, for the creep-fatigue reliability assessment of turbine rotor to legitimately tackle with the large-dynamicity and high-nonlinearity issues induced by multi-physical uncertainties and multi-model uncertainties. To build an accurate MSCA model and accomplish precise assessment, Bayesian regularization - variable metric (BR-VM) error control technique is applied to find the optimal parameters of DNNS model, distributed collaborative strategy is employed to further reduce the complexity of MSCA modeling. The creep-fatigue reliability assessment of turbine rotor in aircraft engine is investigated to check the effectiveness of the developed MSCA. Some conclusions are summarized as follows:

(1) From the creep-fatigue reliability assessment, we acquire the simulation histories and distribution traits of turbine rotor creep-fatigue life, and the creep-fatigue reliable life 629 cycles is advised for creep-fatigue life design of turbine rotor, which is conductive to ensure reliability performance and security assurance of turbine rotor during the service lifetime.

(2) From the creep-fatigue sensitivity analysis, we discover that the dynamic operating loads (rotor speed and body temperature) are the primary sensitive parameters on mean stress and strain range, fatigue strength coefficient and holding creep time are major stochastic factors on creep-fatigue reliable life. These variables are worth of being considered with the highest priority in turbine rotor creep-fatigue design.

(3) The comparison of methods reveals that the presented MSCA possesses high efficiency and accuracy in the creep-fatigue reliability assessment of turbine rotor. Meanwhile, the proposed BR-VM error control technique is promising to structure an efficient DNNS model, and the distributed collaborative strategy is also suitable to reduce the complexity and nonlinearity of turbine rotor creep-fatigue reliability assessment.

REFERENCES

[1] S.-P. Zhu, Q. Liu, Q. Lei, and Q. Wang, "Probabilistic fatigue life prediction and reliability assessment of a high pressure turbine disc considering load variations," *Int. J. Damage Mech.*, vol. 27, no. 10, pp. 1569–1588, Nov. 2018.

[2] P. Yu, D. Zhang, Y. Ma, and J. Hong, "Dynamic modeling and vibration characteristics analysis of the aero-engine dual-rotor system with fan blade out," *Mech. Syst. Signal Process.*, vol. 106, pp. 158–175, Jun. 2018.

[3] P. Gaetani, G. Persico, and A. Spinelli, "Coupled effect of expansion ratio and blade loading on the aerodynamics of a high-pressure gas turbine," *Appl. Sci.*, vol. 7, no. 3, p. 259, Mar. 2017.

[4] L.-K. Song, C.-W. Fei, J. Wen, and G.-C. Bai, "Multi-objective reliability-based design optimization approach of complex structure with multi-failure modes," *Aerosp. Sci. Technol.*, vol. 64, pp. 52–62, May 2017.

[5] Z. Zhan, H. Li, and K. Y. Lam, "Development of a novel fatigue damage model with AM effects for life prediction of commonly-used alloys in aerospace," *Int. J. Mech. Sci.*, vol. 155, pp. 110–124, May 2019.

[6] L.-K. Song, G.-C. Bai, and C.-W. Fei, "Multi-failure probabilistic design for turbine bladed disks using neural network regression with distributed collaborative strategy," *Aerosp. Sci. Technol.*, vol. 92, pp. 464–477, Sep. 2019.

[7] S. L. Sheng and H. Almstedt, "Application of an advanced creep-fatigue procedure for flexible design of steam turbine rotors based on fracture mechanics methods," *J. Eng. Gas. Turb. Power*, vol. 173, no. 3, Mar. 2015. Art. no. 032506.

[8] Z. X. Zhan, "Experiments and numerical simulations for the fatigue behavior of a novel TA2-TA15 titanium alloy fabricated by laser melting deposition," *Int. J. Fatigue*, vol. 121, pp. 20–29, Apr. 2019.

[9] S. Barella, M. Bellogini, M. Boniardi, and S. Cincera, "Failure analysis of a steam turbine rotor," *Eng. Failure Anal.*, vol. 18, no. 6, pp. 1511–1519, Sep. 2011.

[10] W. M. Payten, D. W. Dean, and K. U. Snowden, "A strain energy density method for the prediction of creep-fatigue damage in high temperature components," *Mater. Sci. Eng., A*, vol. 527, nos. 7–8, pp. 1920–1925, Mar. 2010.

[11] S.-P. Zhu, H.-Z. Huang, L.-P. He, Y. Liu, and Z. Wang, "A generalized energy-based fatigue–creep damage parameter for life prediction of turbine disk alloys," *Eng. Fract. Mech.*, vol. 90, pp. 89–100, Aug. 2012.

[12] S.-P. Zhu, Y.-J. Yang, H.-Z. Huang, Z. Q. Lv, and H.-K. Wang, "A unified criterion for fatigue–creep life prediction of high temperature components," *Proc. Inst. Mech. Eng., G, J. Aerosp. Eng.*, vol. 231, no. 4, pp. 677–688, Apr. 2017.

[13] Y. Takahashi, B. Dogan, and D. Gandy, "Systematic evaluation of creep-fatigue life prediction methods for various alloys," *J. Pressure Vessel Technol.*, vol. 135, no. 6, Dec. 2013. Art. no. 061204.

[14] C.-Y. Zhang, Z.-S. Yuan, Z. Wang, C.-W. Fei, and C. Lu, "Probabilistic fatigue/creep optimization of turbine bladed disk with fuzzy multi-extremum response surface method," *Materials*, vol. 12, no. 20, Oct. 2019. Art. no. 3367.

[15] Y. Appalanaidu and S. Gupta, "Probabilistic damage estimation in piping components against thermal creep and fatigue," *Nucl. Eng. Des.*, vol. 273, pp. 202–214, Jul. 2014.

[16] M. Guida and F. Penta, "A Bayesian analysis of fatigue data," *Struct. Saf.*, vol. 32, no. 1, pp. 64–76, Jan. 2010.

[17] Y. Zhao, "A fatigue reliability analysis method including super long life regime," *Int. J. Fatigue*, vol. 35, no. 1, pp. 79–90, Feb. 2012.

[18] B. J. Leira, "Probabilistic assessment of weld fatigue damage for a non-linear combination of correlated stress components," *Probabilistic Eng. Mech.*, vol. 26, no. 3, pp. 492–500, Jul. 2011.

[19] S.-P. Zhu, Q. Liu, W. Peng, and X.-C. Zhang, "Computational-experimental approaches for fatigue reliability assessment of turbine bladed disks," *Int. J. Mech. Sci.*, vols. 142–143, pp. 502–517, Jul. 2018.

[20] D. Meng, S. Yang, Y. Zhang, and S. Zhu, "Structural reliability analysis and uncertainties-based collaborative design and optimization of turbine blades using surrogate model," *Fatigue Fract. Eng. Mater. Struct.*, vol. 42, no. 6, pp. 1219–1227, Aug. 2018.

[21] S.-P. Zhu, H.-Z. Huang, W. Peng, H.-K. Wang, and S. Mahadevan, "Probabilistic physics of failure-based framework for fatigue life prediction of aircraft gas turbine discs under uncertainty," *Rel. Eng. Syst. Saf.*, vol. 146, pp. 1–12, Feb. 2016.

[22] M. P. Enright, S. J. Hudak, R. C. McClung, and H. R. Millwater, "Application of probabilistic fracture mechanics to prognosis of aircraft engine components," *AIAA J.*, vol. 44, no. 2, pp. 311–316, Feb. 2006.

[23] W. A. Grell and P. J. Laz, "Probabilistic fatigue life prediction using AFGROW and accounting for material variability," *Int. J. Fatigue*, vol. 32, no. 7, pp. 1042–1049, Jul. 2010.

[24] L. Morse, Z. S. Khodaei, and M. H. Aliabadi, "A multi-fidelity modelling approach to the statistical inference of the equivalent initial flaw size distribution for multiple-site damage," *Int. J. Fatigue*, vol. 120, pp. 329–341, Mar. 2019.

[25] E. Asaadi and P. S. Heyns, "A computational framework for Bayesian inference in plasticity models characterisation," *Comput. Methods Appl. Mech. Eng.*, vol. 321, pp. 455–481, Jul. 2017.

[26] S. P. Zhu, Q. Liu, J. Zhou, and Z. Y. Yu, "Fatigue reliability assessment of turbine discs under multi-source uncertainties," *Fatigue Fract. Eng. Mater. Struct.*, vol. 41, no. 6, pp. 1291–1305, Jan. 2018.

[27] C.-W. Fei, C. Lu, and R. P. Liem, "Decomposed-coordinated surrogate modeling strategy for compound function approximation in a turbine-blisk reliability evaluation," *Aerosp. Sci. Technol.*, vol. 95, Dec. 2019, Art. no. 105466.

[28] W. Hu, K. K. Choi, and H. Cho, "Reliability-based design optimization of wind turbine blades for fatigue life under dynamic wind load uncertainty," *Struct. Multidisciplinary Optim.*, vol. 54, no. 4, pp. 953–970, Apr. 2016.

[29] C. Lu, Y.-W. Feng, C.-W. Fei, and S.-Q. Bu, "Improved decomposed-coordinated kriging modeling strategy for dynamic probabilistic analysis of multicomponent structures," *IEEE Trans. Rel.*, to be published, doi: 10.1109/TR.2019.2954379.

[30] L.-K. Song, G.-C. Bai, C.-W. Fei, and J. Wen, "Reliability-based fatigue life prediction for complex structure with time-varying surrogate modeling," *Adv. Mater. Sci. Eng.*, vol. 2018, pp. 1–16, Oct. 2018.

[31] U. Alibrandi, N. Impollonia, and G. Ricciardi, "Probabilistic eigenvalue buckling analysis solved through the ratio of polynomial response surface," *Comput. Methods Appl. Mech. Eng.*, vol. 199, nos. 9–12, pp. 450–464, Jan. 2010.

[32] H. Gao, C. Fei, G. Bai, and L. Ding, "Reliability-based low-cycle fatigue damage analysis for turbine blade with thermo-structural interaction," *Aerosp. Sci. Technol.*, vol. 49, pp. 289–300, Feb. 2016.

[33] J. Feng, L. Liu, D. Wu, G. Li, M. Beer, and W. Gao, "Dynamic reliability analysis using the extended support vector regression (X-SVR)," *Mech. Syst. Signal Process.*, vol. 126, pp. 368–391, Jul. 2019.

[34] C. Jin and S.-W. Jin, "Software reliability prediction model based on support vector regression with improved estimation of distribution algorithms," *Appl. Soft Comput..*, vol. 15, pp. 113–120, Feb. 2014.

[35] L.-K. Song, G.-C. Bai, and C.-W. Fei, "Dynamic surrogate modeling approach for probabilistic creep-fatigue life evaluation of turbine disks," *Aerosp. Sci. Technol.*, vol. 95, Dec. 2019, Art. no. 105439.

[36] C. Lu, Y.-W. Feng, C.-W. Fei, and S. Bu, "Decomposed-coordinated framework with enhanced extremum kriging for multicomponent dynamic probabilistic failure analyses," *IEEE Access*, vol. 7, pp. 163287–163300, 2019.

[37] T. V. Santhosh, V. Gopika, A. K. Ghosh, and B. G. Fernandes, "An approach for reliability prediction of instrumentation & control cables by artificial neural networks and Weibull theory for probabilistic safety assessment of NPPs," *Reliab. Eng. Syst. Saf.*, vol. 170, pp. 31–44, Feb. 2018.

[38] X. Wang, S. Wang, J. Tao, G. Sun, and J. Mao, "A PCA–ANN-based inverse design model of stall lift robustness for high-lift device," *Aerosp. Sci. Technol.*, vol. 81, pp. 272–283, Oct. 2018.

[39] A. Heng, S. Zhang, A. C. C. Tan, and J. Mathew, "Rotating machinery prognostics: State of the art, challenges and opportunities," *Mech. Syst. Signal Process.*, vol. 23, no. 3, pp. 724–739, Apr. 2009.

[40] S. Mahadevan and H. Y. Mao, "Probabilistic fatigue-creep life prediction of composites," *J. Reinf. Plast. Comp.*, vol. 23, no. 4, pp. 361–371, 2004.

[41] J. Dong-Mei, S. Jia-Qi, S. Quan, G. Heng-Chao, R. Jian-Xing, and Z. Quan-Jun, "Optimization of start-up scheduling and life assessment for a steam turbine," *Energy*, vol. 160, pp. 19–32, Oct. 2018.

[42] L.-K. Song, C.-W. Fei, G.-C. Bai, and L.-C. Yu, "Dynamic neural network method-based improved PSO and BR algorithms for transient probabilistic analysis of flexible mechanism," *Adv. Eng. Inform.*, vol. 33, pp. 144–153, Aug. 2017.

[43] C.-W. Fei, Y.-S. Choy, D.-Y. Hu, G.-C. Bai, and W.-Z. Tang, "Dynamic probabilistic design approach of high-pressure turbine blade-tip radial running clearance," *Nonlinear Dyn.*, vol. 86, no. 1, pp. 205–223, Jun. 2016.

[44] G. C. Cawley and N. L. C. Talbot, "Preventing over-fitting during model selection via Bayesian regularization of the hyper-parameters," *J. Mach. Learn. Res.*, vol. 8, pp. 841–861, Apr. 2007.

[45] D. Q. Yan, Q. Zhou, J. Z. Wang, and N. Zhang, "Bayesian regularization neural network based on artificial intelligence optimization," *Int. J. Prod. Res.*, vol. 55, no. 8, pp. 2266–2287, 2017.

[46] L. Lukšan and E. Spedicato, "Variable metric methods for unconstrained optimization and nonlinear least squares," *J. Comput. Appl. Math.*, vol. 124, nos. 1–2, pp. 61–95, Dec. 2000.

[47] A. Pourshaghaghy, F. Kowsary, and A. Behbahaninia, "Comparison of four different versions of the variable metric method for solving inverse heat conduction problems," *Heat Mass Transf.*, vol. 43, no. 3, pp. 285–294, Mar. 2006.

[48] L.-K. Song, J. Wen, C.-W. Fei, and G.-C. Bai, "Distributed collaborative probabilistic design of multi-failure structure with fluid-structure interaction using fuzzy neural network of regression," *Mech. Syst. Signal Process.*, vol. 104, pp. 72–86, May 2018.

[49] L.-K. Song, G.-C. Bai, and C.-W. Fei, "Probabilistic LCF life assessment for turbine discs with DC strategy-based wavelet neural network regression," *Int. J. Fatigue*, vol. 119, pp. 204–219, Feb. 2019.

[50] Z.-J. Shi, S. Wang, and Z. Xu, "The convergence of conjugate gradient method with nonmonotone line search," *Appl. Math. Comput.*, vol. 217, no. 5, pp. 1921–1932, Nov. 2010.

[51] S.-P. Zhu, S. Xu, M.-F. Hao, D. Liao, and Q. Wang, "Stress-strain calculation and fatigue life assessment of V-shaped notches of turbine disk alloys," *Eng. Failure Anal.*, vol. 106, Dec. 2019, Art. no. 104187.

[52] H.-J. Kim, "Assessment of creep life fraction for in-service high-temperature components," *Eng. Failure Anal.*, vol. 12, no. 4, pp. 578–585, Aug. 2005.

[53] H. Mao, "Reliability analysis of creep–fatigue failure," *Int. J. Fatigue*, vol. 22, no. 9, pp. 789–797, Oct. 2000.

[54] D. Hu and R. Wang, "Experimental study on creep–fatigue interaction behavior of GH4133B superalloy," *Mater. Sci. Eng., A*, vol. 515, nos. 1–2, pp. 183–189, Jul. 2009.

LU-KAI SONG was born in Heze, China, in 1990. He received the B.S. degree in mechanical engineering and automation from Shandong Jiaotong University, China, in 2013, and the M.S. degree in mechanical design and theory from the Harbin University of Science and Technology, China, in 2015. He is currently pursuing the Ph.D. degree with the School of Energy and Power Engineering, Beihang University.

He is the author of more than 20 articles, including *Advanced Engineering Informatics*, *Mechanical Systems and Signal Processing*, and the *International Journal of Fatigue*. He also holds six national patents. His research interests include surrogate modeling, reliability assessment, probabilistic fatigue design, and multidisciplinary design optimization with machine/deep learning for aircraft engines. He is a Reviewer of more than ten journals such as IEEE Access, *Aerospace Science and Technology*, and *Reliability Engineering and System Safety*.

GUANG-CHEN BAI was born in Harbin, in 1962. He received the B.S. degree in mechanical design and theory from the Harbin University of Science and Technology, China, in 1983, and the Ph.D. degree in structural reliability assessment from the Harbin Institute of Technology, China, in 1993.

From 1993 to 1995, he was an Assistant Professor with the School of Astronautics, Harbin Institute of Technology. From 1995 to 2000, he was an Associate Professor with the School of Energy and Power Engineering, Beihang University. From 2000 to 2016, he was a Professor with the School of Energy and Power Engineering, Beihang University. Since 2016, he has been a Tenured Professor with the School of Energy and Power Engineering, Beihang University. He is the author of more than 100 articles. His research interests include fatigue reliability assessment, vibration reliability evaluation, and multidisciplinary design optimization. He was a member of the American Institute of Aeronautics and Astronautics (AIAA) and the Chinese Society of Aeronautics and Astronautics (CSAA). He is a Reviewer of more than 20 journals such as the *Chinese Journal of Aeronautics*, *Reliability Engineering and System Safety*, and the *Chinese Journal of Mechanical Engineering*.